Lifetime distribution of spontaneous emission from emitter(s) in three-dimensional woodpile photonic crystals

Jing-Feng Liu,[1,3] Hao-Xiang Jiang,[1] Zong-Song Gan,[2] Bao-Hua Jia,[2] Chong-Jun Jin,[1] Xue-Hua Wang,[1,4] and Min Gu[2,5]

[1]*State Key Laboratory of Optoelectronic Materials and Technologies, School of Physics & Engineering, Sun Yat-Sen University, Guangzhou 510275, China*
[2]*Centre for Micro-Photonics and CUDOS, Faculty of Engineering and Industrial Sciences, Swinburne University of Technology, Hawthorn, Victoria 3122, Australia*
[3]*College of Science, South China Agriculture University, Guangzhou 510642, China*
[4]*wangxueh@mail.sysu.edu.cn*
[5]*mgu@swin.edu.cn*

Abstract: Spontaneous emission lifetime distribution in the basic unit cell or on a plane of the excited emitters embedded in woodpile photonics crystals with low refractive index contrast are investigated. It is found that the spontaneous emission lifetime distribution strongly depends on the position and transition frequency of the emitters, and has the same symmetry as that of the unit cell. The lifetimes of emitters near the upper gap edge are longer than that in the center of the pseudo-gap, which is quite a contrast to the conventional concept. Furthermore, it is revealed that the polarization orientation of the emitters has significant influence on the lifetime distribution, and may result in a high anisotropy factor (defined as the difference between the maximum and minimum values of the lifetime) up to 4.2. These results may be supplied in probing the lifetime distribution or orientation-dependent local density of states in future experiments.

OCIS codes: (230.5298) Photonic crystals; (270.0270) Quantum optics.

References and links

1. E. Yablonovitch, "Inhibited spontaneous emission in solid-state physics and electronics," Phys. Rev. Lett. **58**(20), 2059–2062 (1987).
2. S. John, "Strong localization of photons in certain disordered dielectric superlattices," Phys. Rev. Lett. **58**(23), 2486–2489 (1987).
3. E. P. Petrov, V. N. Bogomolov, I. I. Kalosha, and S. V. Gaponenko, "Spontaneous emission of organic molecules embedded in a photonic crystal," Phys. Rev. Lett. **81**(1), 77–80 (1998).
4. M. Megens, J. E. G. J. Wijnhoven, A. Lagendijk, and W. L. Vos, "Fluorescence lifetimes and linewidths of dye in photonic crystals," Phys. Rev. A **59**(6), 4727–4731 (1999).
5. S. John and J. Wang, "Quantum optics of localized light in a photonic band gap," Phys. Rev. B Condens. Matter **43**(16), 12772–12789 (1991).
6. S. Bay, P. Lambropoulos, and K. Mølmer, "Fluorescence into flat and structured radiation continua: an atomic density matrix without a master equation," Phys. Rev. Lett. **79**(14), 2654–2657 (1997).
7. S.-Y. Zhu, Y. Yang, H. Chen, H. Zheng, and M. S. Zubairy, "Spontaneous radiation and lamb shift in three-dimensional photonic crystals," Phys. Rev. Lett. **84**(10), 2136–2139 (2000).
8. H.-G. Park, S.-H. Kim, S.-H. Kwon, Y.-G. Ju, J.-K. Yang, J.-H. Baek, S.-B. Kim, and Y.-H. Lee, "Electrically driven single-cell photonic crystal laser," Science **305**(5689), 1444–1447 (2004).
9. K. Hennessy, A. Badolato, M. Winger, D. Gerace, M. Atatüre, S. Gulde, S. Fält, E. L. Hu, and A. Imamoğlu, "Quantum nature of a strongly coupled single quantum dot-cavity system," Nature **445**(7130), 896–899 (2007).
10. J. J. Wierer, A. David, and M. M. Megens, "III-nitride photonic-crystal light-emitting diodes with high extraction efficiency," Nat. Photonics **3**(3), 163–169 (2009).
11. X.-H. Wang, R. Wang, B.-Y. Gu, and G.-Z. Yang, "Decay distribution of spontaneous emission from an assembly of atoms in photonic crystals with pseudogaps," Phys. Rev. Lett. **88**(9), 093902 (2002).
12. X.-H. Wang, B.-Y. Gu, R. Wang, and H.-Q. Xu, "Decay kinetic properties of atoms in photonic crystals with absolute gaps," Phys. Rev. Lett. **91**(11), 113904 (2003).
13. Z.-Y. Li, L.-L. Lin, and Z.-Q. Zhang, "Spontaneous emission from photonic crystals: full vectorial calculations," Phys. Rev. Lett. **84**(19), 4341–4344 (2000).

14. K. M. Ho, C. T. Chan, C. M. Soukoulis, R. Biswas, and M. Sigalas, "Photonic band gaps in three dimensions: new layer-by-layer periodic structures," Solid State Commun. **89**(5), 413–416 (1994).
15. S. Y. Lin, J. G. Fleming, D. L. Hetherington, B. K. Smith, R. Biswas, K. M. Ho, M. M. Sigalas, W. Zubrzycki, S. R. Kurtz, and J. Bur, "A three-dimensional photonic crystal operating at infrared wavelengths," Nature **394**(6690), 251–253 (1998).
16. S. Noda, K. Tomoda, N. Yamamoto, and A. Chutinan, "Full three-dimensional photonic bandgap crystals at near-infrared wavelengths," Science **289**(5479), 604–606 (2000).
17. K. Aoki, H. T. Miyazaki, H. Hirayama, K. Inoshita, T. Baba, K. Sakoda, N. Shinya, and Y. Aoyagi, "Microassembly of semiconductor three-dimensional photonic crystals," Nat. Mater. **2**(2), 117–121 (2003).
18. J. Li, B. Jia, G. Zhou, C. Bullen, J. Serbin, and M. Gu, "Spectral redistribution in spontaneous emission from quantum-dot-infiltrated 3D woodpile photonic crystals for telecommunications," Adv. Mater. (Deerfield Beach Fla.) **19**(20), 3276–3280 (2007).
19. M. Gu, B. Jia, J. Li, and M. J. Ventura, "Fabrication of three-dimensional photonic crystals in quantum-dot-based materials," Laser Photon. Rev. **4**(3), 414–431 (2010).
20. S. Takahashi, K. Suzuki, M. Okano, M. Imada, T. Nakamori, Y. Ota, K. Ishizaki, and S. Noda, "Direct creation of three-dimensional photonic crystals by a top-down approach," Nat. Mater. **8**(9), 721–725 (2009).
21. K. Ishizaki and S. Noda, "Manipulation of photons at the surface of three-dimensional photonic crystals," Nature **460**(7253), 367–370 (2009).
22. M. J. Ventura and M. Gu, "Engineering spontaneous emission in a quantum-dot-doped polymer nanocomposite with three-dimensional photonic crystals," Adv. Mater. (Deerfield Beach Fla.) **20**(7), 1329–1332 (2008).
23. L. Tang and T. Yoshie, "High-Q hybrid 3D-2D slab-3D photonic crystal microcavity," Opt. Lett. **35**(18), 3144–3146 (2010).
24. A. Tandaechanurat, S. Ishida, D. Guimard, M. Nomura, S. Iwamoto, and Y. Arakawa, "Lasing oscillation in a three-dimensional photonic crystal nanocavity with a complete bandgap," Nat. Photonics **5**(2), 91–94 (2011).
25. R. Wang, X.-H. Wang, B.-Y. Gu, and G.-Z. Yang, "Local density of states in three-dimensional photonic crystals: calculation and enhancement effects," Phys. Rev. B **67**(15), 155114 (2003).
26. M. D. Birowosuto, S. E. Skipetrov, W. L. Vos, and A. P. Mosk, "Observation of spatial fluctuations of the local density of states in random photonic media," Phys. Rev. Lett. **105**(1), 013904 (2010).
27. V. Krachmalnicoff, E. Castanié, Y. De Wilde, and R. Carminati, "Fluctuations of the local density of states probe localized surface plasmons on disordered metal films," Phys. Rev. Lett. **105**(18), 183901 (2010).
28. K. Busch and S. John, "Photonic band gap formation in certain self-organizing systems," Phys. Rev. E Stat. Phys. Plasmas Fluids Relat. Interdiscip. Topics **58**(3), 3896–3908 (1998).
29. I. S. Nikolaev, W. L. Vos, and A. F. Koenderink, "Accurate calculation of the local density of optical states in inverse-opal photonic crystals," J. Opt. Soc. Am. B **26**(5), 987–997 (2009).
30. J.- Liu and X.-H. Wang, "Spontaneous emission in micro- and nano-structures," Front. Phys. China **5**(3), 245–259 (2010).
31. Q. Wang, S. Stobbe, H. Thyrrestrup, H. Hofmann, M. Kamp, T. W. Schlereth, S. Höfling, and P. Lodahl, "Highly anisotropic decay rates of single quantum dots in photonic crystal membranes," Opt. Lett. **35**(16), 2768–2770 (2010).
32. H. J. Monkhorst and J. D. Pack, "Special points for Brillouin-zone integrations," Phys. Rev. B **13**(12), 5188–5192 (1976).
33. W. L. Vos, A. F. Koenderink, and I. S. Nikolaev, "Orientation-dependent spontaneous emission rates of a two-level quantum emitter in any nanophotonic environment," Phys. Rev. A **80**(5), 053802 (2009).

Since the pioneer work of Yablonovich [1] and John [2], the control of spontaneous emission (SE) of emitters with three-dimensional (3D) photonic crystals (PCs) has been extensively investigated [3–7] due to its importance in both fundamental quantum optics research and developing quantum-optical devices, such as low-threshold lasers [8], single-photons sources [9], and light-emitting diodes [10]. One of the most important features of PCs is the photonic band gaps (PBGs). Within the PBGs, the local density of states (LDOS) of electromagnetic waves is suppressed. So the SE is inhibited, leading to a prolonged lifetime of an emitter embedded in the PCs. However, since the LDOS near the band edge is significantly large, a decrease in the lifetime of an emitter is anticipated.

It is well known that the SE has a strong environment-dependent characteristic, which is a basic topic on light-matter interaction in quantum optics. In theory, isotropic and anisotropic dispersion models were put forward to interpret the SE in PCs, respectively, and have already achieved success to different extent [5,7]. But these two models introduced a simple dispersion relation of photons, which inevitably led to some inaccurate results. Wang *et al* [11,12]and Li [13] proposed a full vectorial model to investigate the lifetime of SE within the framework of quantum electrodynamics, which gave a good explanation of the lifetime in experiments.

Recently, researches interests in a woodpile structure [14] have increased dramatically because of the ease in fabrication for woodpile structures [15–20]. Ishizaki and Noda [21]

showed experimentally that the photons can be manipulated at the surface of the woodpile structure. Their work represented an important step in realizing a new route for the manipulation of photons by 3D PCs, as well as establishing the surface science of 3D PCs. In the quantum-dot-infiltrated 3D polymer woodpile structure [18,22], Gu *et al*, for the first time, observed significant modifications in both the emission spectra and SE lifetime in the near-infrared regions. Tang and Yoshie [23] placed woodpile structures on the top and bottom surfaces of a slab including L1 defects. In their work, enhancement of the Q factor without affecting the mode volume and mode frequency was demonstrated. Recently, Arakawa [24] demonstrated, for the first time, lasing oscillation in a three-dimensional woodpile photonic crystals with nanocavity.

However, to our best knowledge, seldom theoretical work with full vectorial method has been conducted to study the SE lifetime distribution and the decay kinetics of a mass of emitters in woodpile structures. In this paper, we study the decay kinetics of the emitters in the woodpile structure that resembles the polymeric PCs fabricated from direct laser writing [18], using the lifetime distribution function (LDF) methods proposed by Wang *et al* [11,25]. The photonic orientation-averaged LDOS (OALDOS) in the woodpile structures are calculated to obtain lifetime distribution. Furthermore, the SE lifetime surface was evaluated based upon the orientation-dependent LDOS (ODLDOS), which opens a new avenue to study the emission dynamics of emitters in PCs. Our theoretical results may be provided as reference results for probing OALDOS or ODLDOS in time-resolved fluorescence observation [26,27] experiments.

On the other hand, it is worthy to point out that the woodpile structure belongs to the diamond lattice group. In the Face Center Cubic (FCC) and diamond structures with a global basis, the point group correspond to O_h^5 and O_h^7 group, respectively. However, in woodpile structure, the basis is composed of three rods, which has lower operation symmetry than the globule. Thus, different from the 48-fold symmetry of the FCC and diamond structures, there are only 16-fold symmetric operations in the woodpile structure. It is also demonstrated that the symmetry of the woodpile structure has pronounced influence on the lifetime distribution.

We consider a 3D woodpile structure with elliptical rods (refractive-index is 1.552) embedded in air. A sketch of the woodpile structure and the corresponding Brillouin zone are shown in Fig. 1. The distance between four adjacent layers is denoted by **c**. Within each layer, the rods are separated by a distance **d** = 1000 nm, and **c/d** = $\sqrt{2}$. The rods have elliptical cross-sections whose short axis width **w** is 150 nm and long axis width **h** is 375 nm. The parameters we adopted are the same as those in experiment [18]. The crystal has a pseudo-gap from frequencies $0.912(2\pi c/a)$ to $0.950(2\pi c/a)$ along the $\Gamma-Z$ direction and the mid-gap frequency is $0.931(2\pi c/a)$ (a is the lattice constant of the PCs and c is the speed of the light in vacuum).
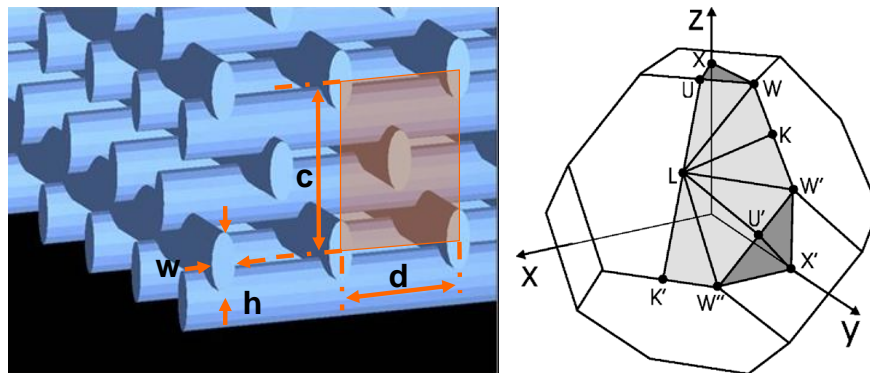

Fig. 1. Sketch of a woodpile structure and the Brillouin zone.

In order to explain the SE lifetime distribution, we defined the LDF as

$$\rho(\tilde{\tau}) = \sum_i W_i \delta(\tilde{\tau} - \tilde{\tau}(\mathbf{r}_i, \omega, \boldsymbol{\mu_d})), \tag{1}$$

where $\tilde{\tau}(\mathbf{r}_i, \omega, \boldsymbol{\mu_d}) = \tau(\mathbf{r}_i, \omega, \boldsymbol{\mu_d}) / \tau_f(\omega)$, $\tau(\mathbf{r}_i, \omega, \boldsymbol{\mu_d})$ is the SE lifetime at a given position $\mathbf{r}_i$ and with a fixed transition dipole moment $\mathbf{d} = d\boldsymbol{\mu_d}$ of an excited emitter in the PCs, $\tau_f(\omega)$ is the SE lifetime in homogeneous medium, and W_i is a weighting factor. Without loss of generality, we chose $W_i = 1$ for the homogeneous distribution of emitters in space. The SE lifetime of an emitter at the position $\mathbf{r}$ is given by

$$\tau(\mathbf{r}, \omega, \boldsymbol{\mu_d}) = [\frac{\pi d^2 \omega_{eg}^2}{3\hbar \varepsilon_0 \omega} \rho_{LDOS}^{OD}(\mathbf{r}, \omega, \boldsymbol{\mu_d})]^{-1}, \tag{2}$$

where ω_{eg} is transition frequency of emitters. $\rho_{LDOS}^{OD}(\mathbf{r}, \omega, \boldsymbol{\mu_d})$ is the ODLDOS that equals to

$$\rho_{LDOS}^{OD}(\mathbf{r}, \omega, \boldsymbol{\mu_d}) = \frac{3}{(2\pi)^3} \sum_n \int_{FBZ} d\mathbf{k} \, | \boldsymbol{\mu_d} \cdot \mathbf{E}_n(\mathbf{k}, \mathbf{r}) |^2 \delta(\omega - \omega_{n\mathbf{k}}), \tag{3}$$

where integration $\mathbf{k}$ vector is over the first Brillouin zone, $\omega_{n\mathbf{k}}$ are the eigenfrequencies, $\mathbf{E}_n(\mathbf{k}, \mathbf{r})$ are the eigenmodes of the structure, and n is the band index.

In the following sections, we consider two scenarios. The first one is the SE from an ensemble of emitters with randomly orientated transition dipoles moments [27]. Accordingly, the OALDOS is [25,28,29]

$$\rho_{LDOS}^{OA}(\mathbf{r}, \omega) = \frac{1}{(2\pi)^3} \sum_n \int_{FBZ} d\mathbf{k} \, | \mathbf{E}_n(\mathbf{k}, \mathbf{r}) |^2 \delta(\omega - \omega_{n\mathbf{k}}). \tag{4}$$

Thus the orientation-averaged LDF equals to [11,30]

$$\rho(\tilde{\tau}) = \sum_i \delta(\tilde{\tau} - \tilde{\tau}(\mathbf{r}_i, \omega)). \tag{5}$$

Secondly we consider that an emitter is placed at a fixed position and has a definite orientation of the transition dipole moment in the inhomogeneous structures [31]. Under such a circumstance, the orientation-dependent LDF can be defined as

$$\rho(\tilde{\tau}) = \sum_{\theta, \varphi} \delta(\tilde{\tau} - \tilde{\tau}(\omega, \boldsymbol{\mu_d}(\theta, \varphi)), \tag{6}$$

where θ and φ are the polar and azimuthal angles.

Equation (2) indicates that the SE lifetime of the emitters depends on the ODLDOS. If the quantity of ODLDOS has been acquired, one may present many quantum characteristics of the emitters interacting with the field in the structured environment. But in experiments, there is no direct method to detect ODLDOS. Accordingly by probing the SE lifetime of the excited emitters, we can acquire the information about the OALDOS. In theory, if we want to get the SE lifetime, we have to calculate the OALDOS or ODLDOS. In Eq. (3) and Eq. (4), the important quantities that determine the ODLDOS or OALDOS are the eigenvalues $\omega_{n\mathbf{k}}$ and the electric field eigenmodes $\mathbf{E}_n(\mathbf{k}, \mathbf{r})$ for each vector $\mathbf{k}$.

The detailed numerical calculation parameters are as following: The first BZ was divided into 16384 coarse grids and 1048576 fine mesh points with the method firstly presented by Monkhorst and Pack [32]. We first calculated the values of the $\mathbf{E}_n(\mathbf{k}, \mathbf{r})$ and $\omega_{n\mathbf{k}}$ on the coarse grids, then we adopted the interpolation methods [32] to obtain the values of the

$\mathbf{E}_n(\mathbf{k},\mathbf{r})$ and $\omega_{n\mathbf{k}}$ on the fine mesh grids. The eigenequation was solved by an expansion of 965 plane waves.

The orientation-averaged lifetime distributions of excited emitters are presented in Fig. 2. We choose three different transition frequencies in each of the Figs. 2(a), 2(b) and 2(c), which correspond to the lower edge, the center and the upper edge of the pseudo-gap, respectively. The reference lifetime τ_0 is selected as the vacuum SE lifetime. In Fig. 2(a), 39668 excited emitters are homogenously distributed on the two elliptic cylinder surfaces that are respectively separated by 3nm and 6nm from the elliptic rod surface outside the rods in a unit cell. In Fig. 2(b) and 2(c), these emitters are distributed on the surface that is far from the elliptic rod surface by 3nm inside and outside the rods, respectively. The results in Figs. 2(a) and 2(b) show that when the emitters are in the air, the SE processes of almost all emitters are accelerated at the lower band edge and the center of the pseudo-gap, but the SE processes of most of emitters are decelerated at the upper band edge. Compared Fig. 2(c) with Figs. 2(a) and 2(b), it can be seen that when the emitters are in the dielectric rods, the lifetime distribution has an obvious change and the SE processes are obviously slowed down. This can be well interpreted by simple physical arguments: the electric displacement component normal to the interface must be continuous when it crosses the interface. This implies the electric field in the dielectric rods is smaller than that in the air. Thus, the larger OALDOS concentrates in the air area.

From the view point of the conventional concept, it is expected that the pseudo-gap may partially inhibit the SE processes, i.e., the lifetime of an emitter in the center of the pseudo-gap should be longer than that near the gap edges. However, Figs. 2(a)–2(c) display that he lifetimes of emitters near the upper gap edge are longer than that in the center of the pseudo-gap that different from the conventional concept. Averagely, we observe that the SE decay processes are in turns slowed down when the transition frequency shifts from the lower band edge to the upper band edge. The physical reason lies in that the SE lifetime of the emitters is determined by all of the electromagnetic field modes in all directions, rather than only by those electromagnetic field modes along the pseudo-gap direction.

Figure 2(d) presents a comparison of the lifetime distribution of emitters in the woodpile structure with that in a FCC structure. Their transition frequencies lie in the pseudo-gap of each structure, respectively. The FCC structure is composed of spherical globules with refractive index 1.552 in air background, and its filling fraction is 0.74. In the calculation of the FCC structure, we used 4700 points on the surface of the globules in a unit cell. The orange line in Fig. 2(d) shows that the decay process for almost all emitters in the FCC structure is remarkably accelerated. This indicates the structure environments have significant effects on the SE lifetime and the decay dynamics of the emitters.
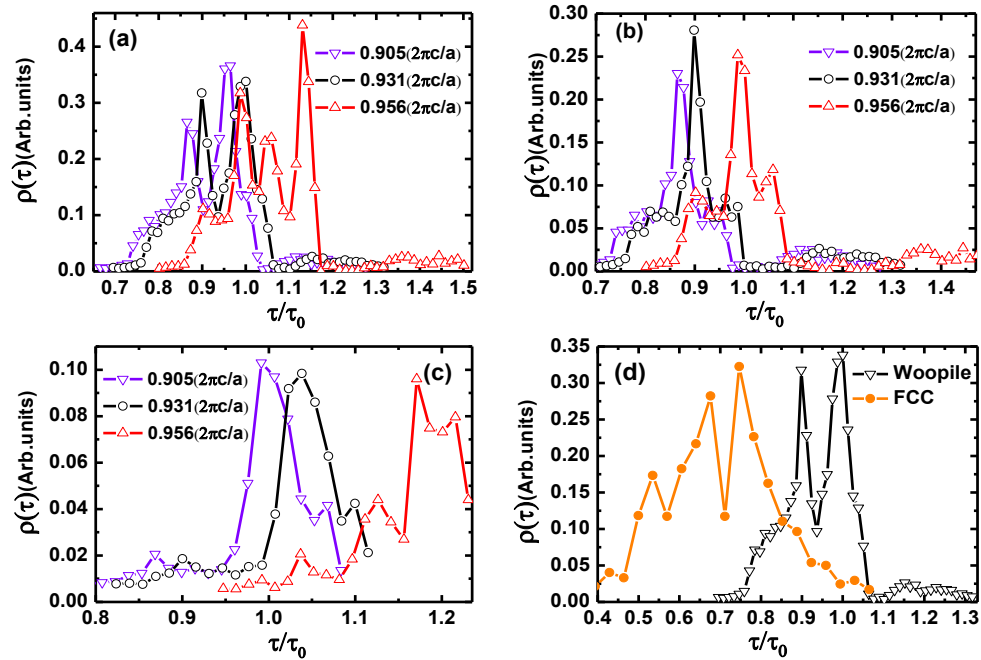
Fig. 2. Averaged lifetime distributions of the emitters in woodpile PCs with different transition frequencies $0.905(2\pi c/a)$, $0.931(2\pi c/a)$ and $0.956(2\pi c/a)$, respectively. (a) for the emitters located on the two surfaces far from the rod surface by 3nm and 6nm outside the elliptical rods, (b) for the emitters distributed on the surface far from the rod surface by 3nm outside the elliptical rods, and (c) for the emitters spread on the surface far from the rod surface by 3nm inside the elliptical rods. (d) The orange line corresponds to the emitters of transition frequency $0.732(2\pi c/a)$ at the surface of the globules in the FCC structure. The black line is the same as that in Fig. 2(a) with the transition frequency $0.931(2\pi c/a)$.

With the development of an accurate positioning technology, the detection can focus on certain planes. Figure 3 reveals the averaged SE lifetime distribution in four planes with z = 0, z = a/4, z = a/2, and z = 3a/4 (a is the lattice constant of the PCs), respectively. The white areas denote the dielectric rods. 61 × 61 points are considered in each plane and other parameters are the same as those in Fig. 2. Figure 3 presents an intuitive picture that the averaged SE lifetime has strong position dependent properties. Moreover, we perceive that the SE lifetime is obviously symmetric with respect to the 45° diagonal line, but it is non-symmetric about the 135° line which is different from that in the diamond structures and FCC structures composed of the global basis. Thus, the results prove that our group operation analysis is correct. In general, the calculated results show that the SE lifetime of many points near the surfaces of the rods speeds up and that of the other points, which are a bit far from the surfaces, slows down.
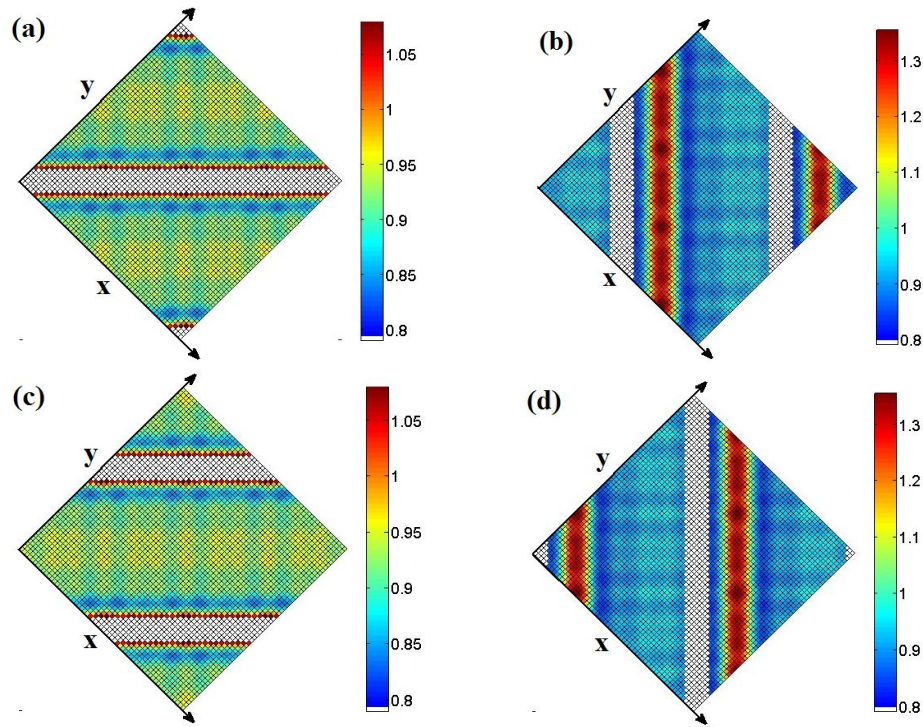
Fig. 3. Averaged lifetime distribution of emitters with a reduced transition frequency 0.658 and lying on the planes (a) z = 0; (b) z = a /4; (c) z = a /2; (d) z = 3a/4.

In the previous paragraphs, we discussed the orientation-averaged SE lifetime in the basic unit cell or in a plane. We have known that the SE lifetime is isotropic in homogeneous dielectrics. Then, how about the emitters in the inhomogeneous dielectrics? To answer this question, we calculate the orientation-dependent SE lifetime surface according to the methods given by Vos [33].

Insets (I) and (II) in Fig. 4(a) show the orientation-dependent SE lifetime surfaces of an emitter with the transition frequency of $0.931(2\pi c/a)$ at two positions (0.055a, 0, 0) and (0, 0.122a, 0.25a) near the outer surfaces of the rods. The SE lifetime surfaces are normalized to the SE lifetime in vacuum. We observe that the SE lifetime surfaces vary significantly with the difference of the positions in space and the orientations of the dipole. In position (I), we find that SE lifetime reaches the maximum when the orientation of the dipole parallel to the axis of the rods. When the orientation of the dipole lies in a plane which is perpendicular to the rods, the lifetime is accelerated. We concluded that the electric fields prefer lying in planes which are perpendicular to the rods. In position (II), there is different orientation-dependent lifetime distribution. To quantify the difference, we defined an SE lifetime anisotropy factor $\eta = \tau_{max}(\theta,\varphi)/\tau_{min}(\theta,\varphi)$. We observe an anisotropy factor of 1.52 and 3.62 at positions (I) and (II), respectively. Besides, the red curve in Fig. 4(a) shows that the SE decay is speeded up in position (I) for almost all orientations of the dipole. However, in position (II), in many dipole orientations, the SE is inhibited and for a few orientations the SE lifetimes are significantly prolonged.

Insets (III) and (IV) in Fig. 4(b) present the orientation-dependent SE lifetime distributions of an emitter with two different frequencies at a fixed position (0.055a, 0, 0). The surface is dumbbell-like and long-bread-like at the frequencies $0.658(2\pi c/a)$ and $0.956(2\pi c/a)$, respectively. Thus, the surfaces are different for different transition frequencies. Moreover, we observe anisotropy factors of 4.22 and 2.53. The curve (IV) shows that the SE lifetime is

decelerated in almost all orientations with frequency $0.956(2\pi c/a)$. According to Fig. 4, we find that the SE lifetime surfaces give a compact representation of the rich behavior of the dependence of the SE lifetime on the dipole orientation.
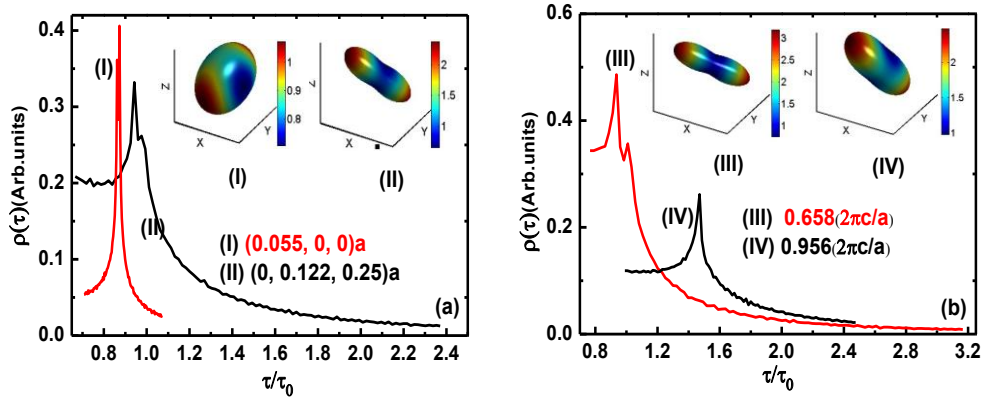

Fig. 4. Orientation-dependent emission lifetime distributions for an emitter at a fixed position in woodpile PCs. (a) Curves (I) and (II) are emission lifetime distributions of an emitter located at the points (0.055a, 0, 0) and (0, 0.122a, 0.25a) at a frequency $0.931(2\pi c/a)$. Insets (I) and (II) are the relative emission lifetime surfaces versus the dipole orientation on the same points and at the same frequency as the curves (I) and (II). (b) Curves (III) and (IV) are emission lifetime distributions of an emitter located at the point (0.055a, 0, 0) at the frequency $0.658(2\pi c/a)$ and $0.956(2\pi c/a)$, respectively. Insets (III) and (IV) are the relative emission lifetime surfaces versus the dipole orientation at the same point and the same frequency as the curves (III) and (IV).

In conclusion, we have investigated the orientation-averaged and orientation-dependent SE lifetime distribution of the excited emitters with different transition frequencies at different positions in the polymer woodpile PCs that fabricated by direct laser writing. It has been demonstrated that there are very wide lifetime distributions of the emitters in the woodpile PCs even for the refractive index contrast low to 1.552. The SE decay processes of the emitters in the air are faster than that in the rods, and the lifetime distribution of the emitters has the same symmetry as the unit cell. Different from the conventional concept, emitters with emission frequency near the upper gap edge have longer lifetime than that in the center of the pseudo-gap. It has also been revealed that the SE lifetime strongly depends on the transition dipole orientation of the emitters. This leads to the anisotropy surface of the lifetime distribution, and the maximum anisotropy factor may be high up to 4.2. These results may be supplied in probing the lifetime distribution or ODLDOS for the future experiments that can be done in the polymer woodpile structures.

Acknowledgments